

## Fabrication of large-scale zinc oxide ordered pore arrays with controllable morphology

Bingqiang Cao,<sup>a</sup> Weiping Cai,<sup>\*a</sup> Fengqiang Sun,<sup>a</sup> Yue Li,<sup>a</sup> Yong Lei<sup>b</sup> and Lide Zhang<sup>a</sup>

<sup>a</sup> Key Lab of Materials Physics, Institute of Solid State Physics, Chinese Academy of Sciences, Hefei, 230031, Anhui, P.R. China. E-mail: wpcai@issp.ac.cn; Fax: +86-551-5591434

<sup>b</sup> Singapore-MIT Alliance, National University of Singapore, 04-10, 4 Engineering Drive 3, 117576, Singapore

Received (in Cambridge, UK) 22nd March 2004, Accepted 17th May 2004

First published as an Advance Article on the web 17th June 2004

The fabrication of large-scale ZnO ordered pore arrays by the potentiostatic electrochemical deposition method based on a two-dimensional ordered colloidal monolayer template is reported. The pore morphology evolves from hemispherical to a well-like structure by controlling the deposition potential.

Two-dimensional (2D) ordered pore arrays (films) have a high specific surface area and an ordered arrangement of pores, and they may have novel applications in catalysis, gas sensors, optoelectronic devices, membrane and cell culture.<sup>1–4</sup> Many methods such as electron-beam lithography,<sup>5</sup> nanosphere lithography,<sup>6</sup> microcontact printing,<sup>7</sup> and alumina templating<sup>8</sup> have been adopted to fabricate nanopore/nanoring arrays. However, control of the pore morphology is still a challenge. A 2D ordered colloidal monolayer has been used as a new template for this purpose. Yi and Kim have demonstrated its use as a template to fabricate 2D titania honeycomb structures<sup>9</sup> and trigonal polymer nanostructures<sup>10</sup> by sintering rheology and selective dissolution of self-assembled colloidal crystals. Kanungo and Collinson have reported the fabrication of silica nanocavities by mixing the silica sol and polystyrene latex spheres *via* spin-coating.<sup>11</sup> The size and depth of the nanocavities can be controlled by the ratio of silica sol to polystyrene sphere (PS) latex. But this method cannot achieve large-scale ordered nanocavities because silica sol will influence the self-assembling process that is important for the preparation of large-scale colloidal template.<sup>12</sup> Recently, we have demonstrated a simple and universal morphology-controlled growth of large-scale 2D ordered pore arrays based on solution-dipping<sup>13</sup> by changing the precursor concentration.

In this communication, we report a more precise method for synthesizing large-scale (cm<sup>2</sup>) ZnO ordered pore arrays based on a 2D colloidal monolayer template and one-step electrochemical deposition (ECD) technique, in which the pore morphology can be controlled from hemispherical to a well-like structure by controlling the deposition potential.

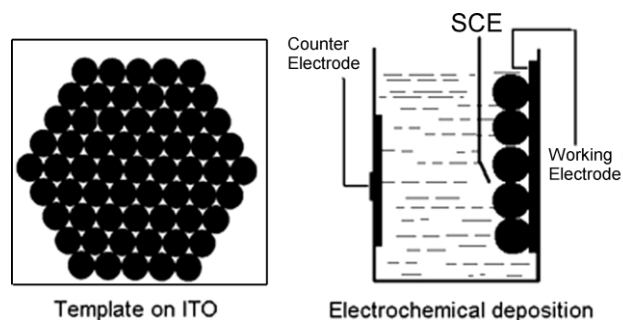
A circular 1 μm PS monolayer colloidal crystal with cm<sup>2</sup> size was prepared on a glass slide by spin-coating and transferred to a conducting ITO-glass substrate, as previously described.<sup>13</sup> The ITO-glass substrate with the monolayer was heated at 350 K for about 3 min to sinter the PSs on the ITO before it was immersed in the electrolyte aqueous zinc nitrate solution (0.05 M) as the working electrode for ECD. A zinc sheet (99.99% purity) acted as the counter electrode. A saturated calomel electrode (SCE) was used as the reference electrode. The deposition device is schematically illustrated in Scheme 1. The deposition temperature was fixed at 355 K in a water bath. The deposition time was 2 h for all samples. Our experiment showed that electrodeposition is very sensitive to the potential and can not occur below 0.8 V (relative to the SCE), which is in agreement with previous reports.<sup>14</sup> When the potential is higher than 1.4 V, the deposition is too fast to be used in our case. In this work, a deposition potential from 1.0 to 1.4 V was applied.

After deposition, the samples were washed with distilled water and then ultrasonically washed in methylene chloride (CH<sub>2</sub>Cl<sub>2</sub>) for about 1 min to dissolve and remove the PSs, followed by washing with distilled water again and drying before further characterizations.

Fig. 1 is the field-emission scanning electronic microscope (FE-SEM) image of a typical 2D colloidal monolayer template, which has been transferred to an ITO-glass substrate and heated at 350 K for 3 min. After electrodeposition and removal of PSs, we can obtain ordered pore arrays. Fig. 2 indicates this structure for the sample under a deposition potential of 1.0 V. The pores are hemispherical in shape and orderly arranged. Further experiments show that the array morphology depends on the deposition potential. With an increase of the potential, the pore skeleton evolves towards a thin wall. When the potential was increased up to 1.4 V, we found that the morphology of the porous film assumes a well-like structure, which is similar to that found in the carbon nanotubes and ZnO nanowire growth processes,<sup>15,16</sup> as illustrated in Fig. 3.

Fig. 4 shows the XRD patterns for such ordered porous films prepared at different ECD potentials of 1.0 V and 1.4 V. The standard data of ZnO is also presented. All diffraction peaks can be identified as hexagonal wurtzite ZnO (JCPDS 36-1451,  $a_0 = 3.253$  Å,  $c_0 = 5.209$  Å) with the measured lattice constants  $a$  and  $c$  of 3.25 and 5.21 Å, respectively ( $c/a = 1.60$ ), which indicates the purity of the sample. In addition, ZnO crystal growth exhibits significant preferential orientation along the [001] crystal axis with increase of the potential.

Recently, the one-step method to electrochemically deposit ZnO film<sup>17</sup> and nanowires<sup>18</sup> has been reported, but the mechanism is not very clear. According to previous discussions,<sup>19</sup> we suggest that the



Scheme 1 Illustration of electrodeposition.

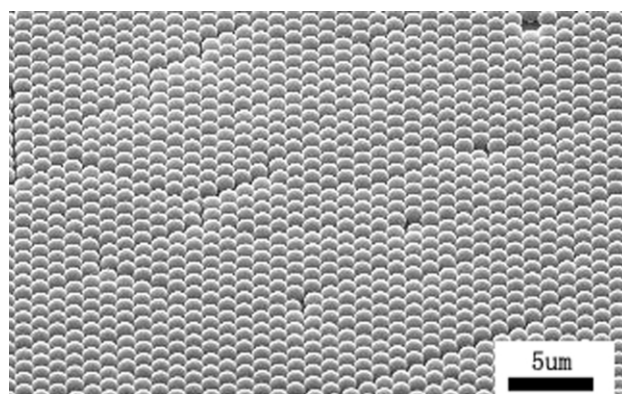
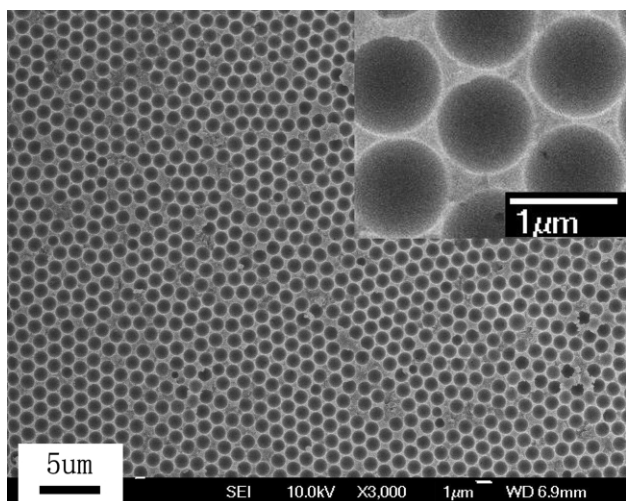
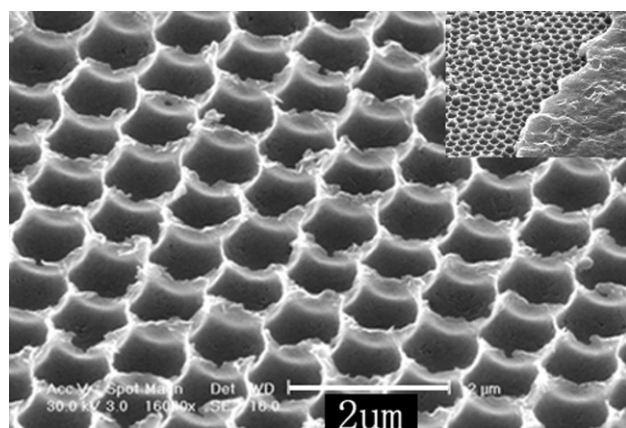


Fig. 1 A typical FE-SEM image of a 2D colloidal monolayer crystal.



**Fig. 2** FE-SEM image of pore arrays under the potential of 1.0 V. Inset: a magnified area.



**Fig. 3** FE-SEM image of pore arrays under the potential of 1.4 V. Inset: ultrasonic washing for a shorter time, (see text).

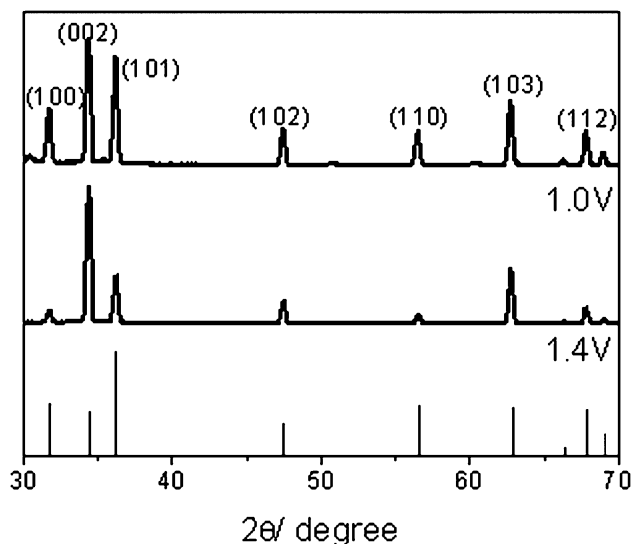


**Fig. 4** XRD patterns for the samples at different potentials.

reduction of the nitrate ( $\text{NO}_3^-$  to  $\text{NO}_2^-$ ) in mild acid solution of  $\text{Zn}^{2+}$ , which results in increase of the pH value near the electrode surface, is crucial. With increasing concentration of  $\text{OH}^-$ ,  $\text{Zn}(\text{OH})_2$

will form and deposit on the cathode electrode. The deposited  $\text{Zn}(\text{OH})_2$  will subsequently decompose and form  $\text{ZnO}$  on the substrate at the temperature of the water bath. The morphology evolution of the  $\text{ZnO}$  ordered pore array with deposition potential could be attributed to the different deposition rate or the growth rate of crystallites when the applied potential was changed. As we all know, the high potential should correspond to a high deposition rate. At a low electrodeposition potential the crystallites on the substrate grew slowly and sufficiently filled the interstices among PSs in the monolayer, leading to hemi-spherical hollow arrays after 2 h deposition and removal of PSs. On the contrary, at a higher potential the crystallites grew rapidly and could not fully fill the interstices, resulting in a nanowall-like structure. Because of the high deposition rate, PSs were completely buried in the deposited film before the interstices were fully filled. Subsequent dissolution of PSs in  $\text{CH}_2\text{Cl}_2$  solution and ultrasonic washing induced the upper part of the film to disconnect at the contact area between adjacent PSs. This has been confirmed in the inset of Fig. 3, which corresponds to the sample in Fig. 3 but with ultrasonic washing for a shorter time (only partially removing the upper film). We can see that the upper part of the film in some areas is still not disconnected. Also, the preferred growth of crystals at the higher potential may be attributed to the rapid deposition rate.

In summary, we have described a simple and more precise strategy for the preparation of large-scale 2D pore arrays with controllable morphology.  $\text{ZnO}$  is an important semiconductor and this nanostructured  $\text{ZnO}$  may have potential practical applications in waveguide ring laser,<sup>20</sup> energy storage or conversion, gas sensor, field emission and biomedical devices.<sup>15</sup> Furthermore, this strategy could also be suitable for other materials such as metals and other compounds.

This work was co-supported by the National Natural Science Foundation of China (grant number: 50271069), and National "863" Project (grant number: 2002AA302614).

## Notes and references

- S. I. Matsushita, T. Miwa, D. Atryk and A. Fujishima, *Langmuir*, 1998, **14**, 6441.
- C. D. Elizabeth, K. V. Oomman and G. O. Keat, *Sensors*, 2002, **2**, 91.
- M. Imada, S. Noda, A. Chutinan and T. Tokuda, *Appl. Phys. Lett.*, 1999, **75**, 316.
- T. Tatsuma, A. Ikezawa and Y. Ohko, *Adv. Mater.*, 2000, **12**, 643.
- T. W. Ebbesen, H. J. Leze and H. F. Ghaemi, *Nature*, 1998, **391**, 667.
- M. Winzer, M. Kleiber, N. Dix and R. Wiesendanger, *Appl. Phys. A: Mater. Sci. Process.*, 1996, **63**, 617.
- Y. Xia, J. Rogers, K. E. Paul and G. M. Whitesides, *Chem. Rev.*, 1999, **99**, 1823.
- K. L. Hobbs, P. R. Larson, G. D. Lian, J. C. Keay and M. B. Johnson, *Nano Lett.*, 2004, **4**, 167.
- D. K. Yi and D. Y. Kim, *Nano Lett.*, 2003, **3**, 207.
- D. K. Yi and D. Y. Kim, *Chem. Commun.*, 2003, **8**, 982.
- M. Kanungo and M. M. Collinson, *Chem. Commun.*, 2004, **5**, 548.
- N. D. Denkov, O. D. Velev, P. A. Kralchevsky, I. B. Ivanov, H. Yoshimura and K. Nagayama, *Langmuir*, 1992, **8**, 3183.
- F. Q. Sun, W. P. Cai, Y. Li, B. Q. Cao, Y. Lei and Lide Zhang, *Adv. Funct. Mater.*, 2004, **14**, 283.
- S. Peulon and D. Lincont, *Adv. Mater.*, 1996, **8**, 166.
- H. T. Ng, J. Li, M. K. Smith, P. Nguyen, A. Cassell, J. Han and M. Meyyappan, *Science*, 2003, **300**, 1249.
- Y. Wu, P. Qiao, T. Chong and Z. Shen, *Adv. Mater.*, 2002, **14**, 64.
- M. Izaki and T. Omi, *Appl. Phys. Lett.*, 1996, **68**, 2439.
- M. J. Zheng, L. Zhang, G. H. Li and W. Z. Shen, *Chem. Phys. Lett.*, 2002, **363**, 123.
- M. Izaki and T. Omi, *J. Electrochem. Soc.*, 1996, **143**, L53.
- S. H. Kim, H. Y. Ryu, H. G. Park, G. H. Kim, Y. S. Choi and Y. H. Lee, *Appl. Phys. Lett.*, 2002, **81**, 2499.